Equating the real and the imaginary parts of (7) results in

$$\frac{2\delta f}{f_0} = \frac{\iiint_{\Delta V} \frac{\omega_p^2}{\omega_0^2} |E_0|^2 dV}{\iiint_V |E_0|^2 dV} \quad (8)$$

and

$$\frac{Q_0 - Q_1}{Q_0 Q_1} = \frac{\iiint_{\Delta V} \frac{\omega_p^2 \nu}{\omega_0^3} |E_0|^2 dV}{\iiint_V |E_0|^2 dV}. \quad (9)$$

Eqs. (8) and (9) are the most general results as they allow for a density variation, hence also a collision frequency variation, both in the transverse and in the longitudinal directions. One could now perform these integrations using an assumed spatial distribution in both the transverse and longitudinal directions.

As an example, consider a uniform density plasma slab of infinite cross section placed in the resonator. One obtains upon integrating (8) and (9)

$$\frac{2\Delta f}{f_0} = \frac{\Delta L}{L} \frac{\omega_p^2}{\omega_0^2} \quad (10)$$

$$\frac{Q_0 - Q_1}{Q_0 Q_1} = -\frac{\Delta L}{L} \frac{\omega_p^2 \nu}{\omega_0^3}. \quad (11)$$

Using the measured change in resonant frequency, (10) may now be solved for the number density. Using the measured change in the cavity Q, (11) will yield the collision frequency. Eq. (10) is identical to (8) of Primich and Hayami with ΔN replaced by $-\omega_p^2/2\omega^2$ which is shown later in their text.

Experimental comparison with Langmuir probe measurements made in a toroidal octupole plasma confinement device[5] verify the above theory. At 10 Gc the resonator measured a number density of 5×10^9 el/cm^3 as also did the probe.

The parameters Δf and f_0 can be measured to a greater precision using a dual mode[6] cavity. The ratio $\Delta f/f_0$ has been measured as 3×10^{-8} at 35 Gc, hence the diagnostic capability in this frequency range would be to measure number densities from 10^6 el/cm^3 to 10^{14} el/cm^3.

The collision frequency relation (9) could alternatively be derived by considering the transmission line analog of a resonant cavity, solving for the attenuation constant which would depend on the collision frequency of such a line, relating it to the Q's of the filled and unfilled cavities, and finally solving for the collision frequency.

K. E. Lonngren
J. W. Mink
J. B. Beyer
Dept. of Elec. Engrg.
University of Wisconsin
Madison, Wis.

[5] W. E. Wilson and D. M. Meade, "Langmuir probe measurements on plasma in a torroidal octupole magnetic field," *Bull. Am. Phys. Soc.*, to be published.
[6] E. H. Scheibe, "Surface Wave and Antenna Engineering Research Study," University of Wisconsin, Madison, Tenth Quarterly Progress Rept., Contract No. DA-36-039-sc-85188; March 31, 1964.

Step-Twist Diode Switch

Two X-band diode switches have been combined with a step-twist waveguide section to form a very compact broad-band step-twist diode switch.

The device shown in Fig. 1 can replace a step twist in a system when it is necessary to add a switch to the system.

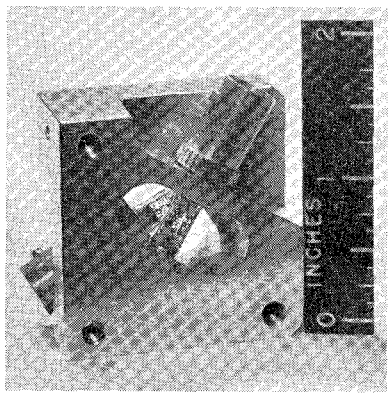

Fig. 1—Step-twist diode switch.

The step twist consists of equal length equiangular twisted sections cut quite inexpensively with a 0.400 inch diameter mill. The VSWR of the step twist alone is shown in Fig. 2.

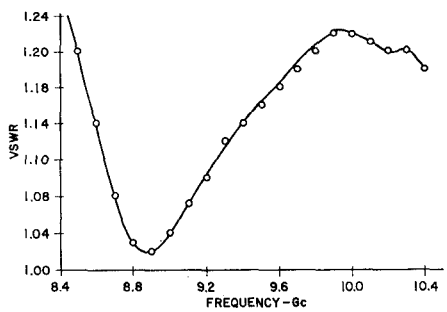

Fig. 2—Step-twist characteristics.

The diode switch consists of two 1N263 diodes centered in each step. The switching voltage is delivered to the diodes through modified BNC connectors. The isolation of two diode switches is a maximum when they are about a quarter wavelength apart. These diodes are a quarter wavelength apart at 10.2 Gc but a capacitive step separates them, lowering the frequency slightly. From Fig. 3 it can be seen that the isolation is greater than 40 db from 8.4 Gc to 10.4 Gc peaking at 9.9 Gc. The insertion loss is less than 3 db from 9.2 Gc to 10.4 Gc. Although the diodes used are limited to switching powers below 50 mw, any of the wide selection of higher power X-band diode switches could be used in this structure.

Manuscript received April 27, 1964.

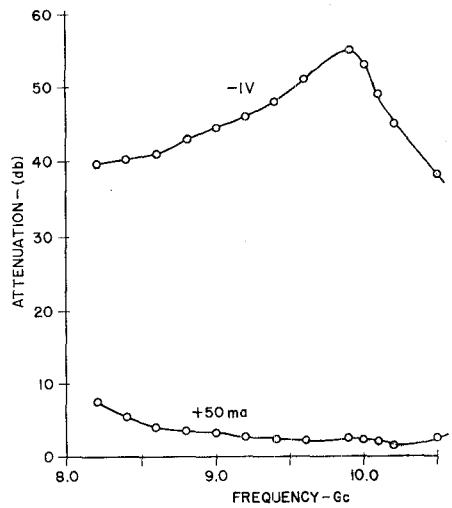

Fig. 3—Frequency dependence of the isolation and insertion loss of the step-twist diode switch.

H. S. Jones, Jr.
R. V. Garver
Harry Diamond Labs.
Washington, D. C.

Dielectric Resonators for Microwave Applications

The purpose of this communication is to report certain test results recently obtained with resonators made of single crystal rutile. Since rutile has a very high dielectric constant and a very low loss factor, microwave resonators made of rutile have several desirable characteristics. Compared to metallic resonators it is possible to reduce the size of the rutile resonator, which is especially useful at lower microwave frequencies. The Q factor of rutile resonators is very high and at room temperature may be of the order of several thousand, while at liquid helium temperature it may even reach 10^5. It can be shown that the ratio of electric and magnetic field strengths of dielectric cavity to metallic cavity is proportional to $(E)^{1/4}$ and $(E)^{3/4}$, respectively. Therefore, with the same available power, an increase in field intensity can be obtained. Furthermore, these fields are not confined to the inside of the rutile resonator but extend beyond the dielectric surface into free space. Because of these characteristics rutile resonators are finding useful applications in traveling-wave masers, in harmonic generators (in conjunction with varactor diodes), in novel RF Hall-effect-devices, and in experiments with parametric superconducting devices.

Manuscript received May 4, 1964. The research reported in this paper was sponsored by the Air Force Cambridge Labs., Office of Aerospace Research, under Contract No. AF19(628)-262, and RCA Labs., Princeton, N. J.

TABLE I

Resonator	Radius	Length	Frequency, Mc Measured	Frequency, Mc Computed
TiO_2	0 050 inch	0.250 inch	5747	5690
TiO_2	0.050 inch	0 110 inch	6250	6280
TiO_2	0.050 inch	0 050 inch	7350	8590
$SrTiO_3$	0.250 inch	0 250 inch	2450	2380

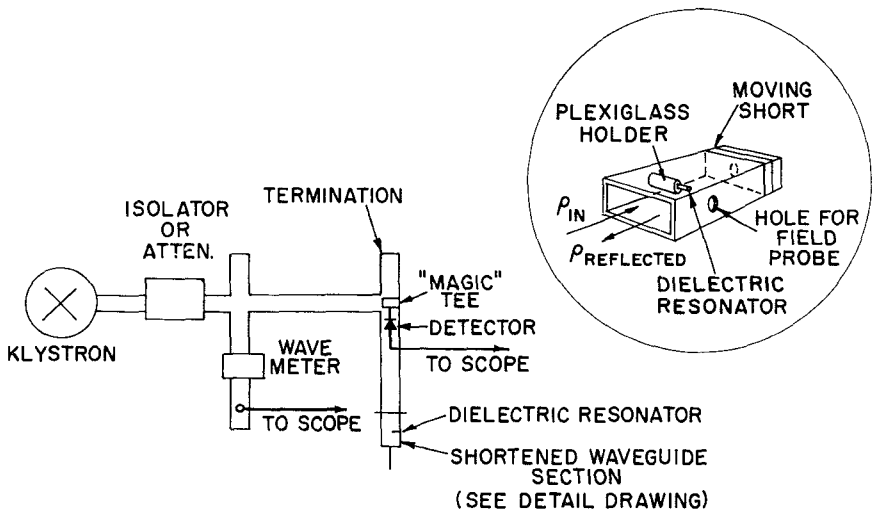

Fig. 1—Experimental setup for measuring Q and fields.

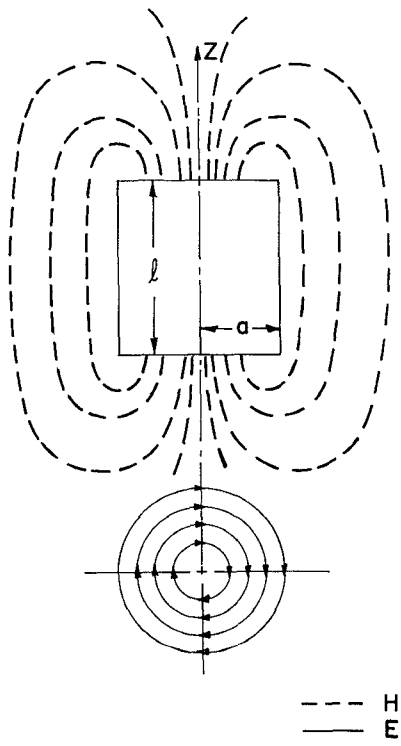

Fig. 2—Magnetic and electric fields for resonant TiO_2 cylindrical cavity.

Table I gives an account of the various cylindrical resonators that we have measured. The analytical expressions for resonant cavities have been well established in the literature [1]–[3]. The dielectric constants which were used in these computations were those given for room temperature [4].

Fig. 1 shows the experimental setup for the field and Q measurements. The rutile resonator is mounted inside a short-circuited waveguide section whose field is employed to excite the resonator. The magic-tee section is used in conjunction with a detector to display the reflections from the shorted waveguide and the dielectric resonator. A sharp dip in the reflected klystron mode indicates the resonance of the dielectric resonator. By replacing the terminated arm of the magic tee with a movable short, the display on the 'scope is inverted, and transmission is seen in place of absorption. The 3-db bandwidth and thus the Q can easily be measured from this display.

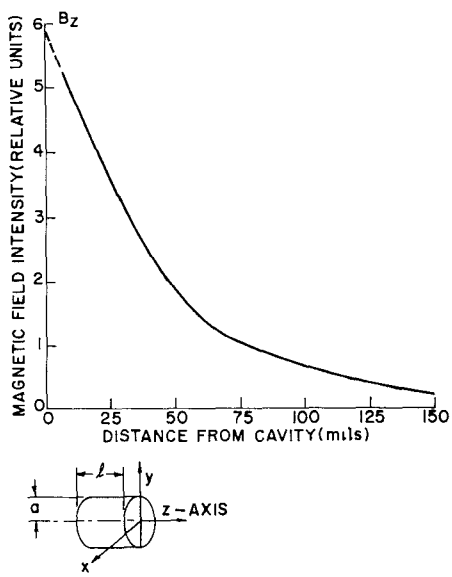

Fig. 3—Intensity of external magnetic field along Z axis.

Tiny H and E probes were used in measuring the external magnetic and electric fields near the face of the cylindrical resonator. The configuration of these fields for the fundamental mode is shown in Fig. 2. It was found that a strong normal magnetic field exists at the face of the cylindrical resonator and that the electric field is circular. These fields are similar to those of a cylindrical metallic cavity in the TE_{011} mode with the electromagnetic field extending into free space. The relative intensity of the magnetic field is mapped in Figs. 3 and 4. Note that the intensity falls off about exponentially with the distance away from the face of the resonator. The maximum external magnetic field intensity of the dielectric resonator was approximately ten times greater than that of a comparable re-entrant metallic cavity, and approximately fifteen times greater than that of the shorted waveguide. It is this concentration of field intensity that makes the dielectric resonator a most promising element for future microwave devices.

The temperature dependence of the dielectric material was observed by noting the change in resonant frequency of the resonator when it was cooled to liquid nitrogen and helium temperatures. Since the dielectric constant increases as the temperature is lowered, the frequency of resonance decreases.

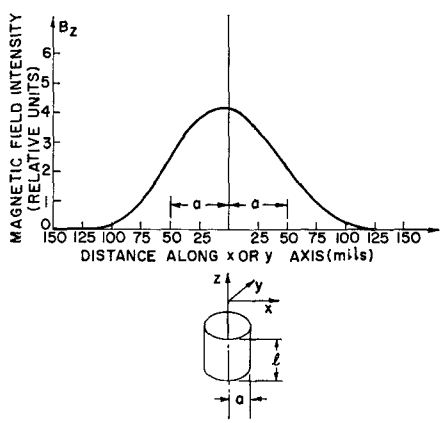

Fig. 4—Intensity of external magnetic field along x or y axis.

ACKNOWLEDGMENT

The authors wish to thank Dr. K. K. N. Chang for his many helpful suggestions during the course of this work.

R. V. D'AIELLO
H. J. PRAGER
RCA Labs.
Princeton, N. J.

REFERENCES

[1] S. Ramo and J. R. Whinnery, "Fields and Waves in Modern Radio," John Wiley and Sons, Inc., New York, N. Y.; 1953.
[2] A. F. Harvey, "Microwave Engineering," Academic Press, London, England, and New York, N. Y.; 1963.
[3] A. Okaya and L. F. Barash, "The dielectric microwave resonator," PROC IRE, vol. 50, pp. 2081–2092; October, 1962.
[4] E. S. Sabisky and H. J. Gerritsen, "Measurements of the dielectric constant of rutile at microwave frequencies between 4.2 and 300°K," *J. Appl. Phys.*, vol. 33, pp. 1450–1453; April, 1962.